This is a previous version of the article published in Journal of Electroanalytical Chemistry. 2017, 793: 34-40. doi:10.1016/j.jelechem.2016.12.044

Enhancement of the direct electron transfer to encapsulated cytochrome c by electrochemical functionalization with a conducting polymer

Sara López-Bernabeu[1], *Alonso Gamero-Quijano*[1], *Francisco Huerta*[2], *Emilia Morallón*[1,*], *Francisco Montilla*[1,*]

[1] Dept. Química Física e Instituto Universitario de Materiales, Universidad de Alicante, Ap. 99, E-03080, Alicante, Spain

[2] Dept. Ingenieria Textil y Papelera, Universitat Politecnica de Valencia, Plaza Ferrandiz y Carbonell, 1. E-03801, Alcoy, Spain

Corresponding authors: morallon@ua.es, francisco.montilla@ua.es

ABSTRACT

The present work deals with the direct electrochemistry of cytochrome c encapsulated within a methyl-modified silica film prepared by the sol-gel method. It was observed that the voltammetric currents of the redox processes grow in proportion to the protein amount inserted within the gel up to a limiting value. From that point, recorded currents remain independent of the amount of protein loaded. Such a behavior indicates that a portion of cyt c molecules is located in non-accessible sites of the silica matrix. The electrochemical insertion of PEDOT through silica pores was carried out to connect those electrically isolated protein molecules and *in situ* UV-vis spectroscopy was used to gain information on the redox process of encapsulated cyt c. It was observed that the presence of conducting polymer gives rise to a 3-fold enhancement in cyt c electrochemical reduction rate at the initial stages of the treatment, irrespective of the amount of inserted polymer. The faster electrochemical reduction rate was obtained after the insertion of 6.45 μg PEDOT within a silica gel containing 0.5 mg protein. The presence of low conductivity domains in the conducting polymer or the hindrance to the protein free movement could explain that higher amounts of inserted PEDOT cannot improve the electrochemical reduction rate.

KEYWORDS: sol-gel, ORMOSIL, cytochrome c, direct electron transfer, conducting polymer, PEDOT-PSS, hybrid silica matrix

1. Introduction

Direct electrochemistry of proteins has become a major subject for the development of biotechnological applications. Electrochemical techniques allow fundamental studies about structural organization (as a function of redox environment) and the study of key mechanisms for electron transfer. Deeper knowledge of these processes would allow the development of more efficient biotechnological devices, such as highly active enzymatic fuel [1–4]or third-generation biosensors[5–7].

A key aspect of these devices is the direct electron transfer (DET) without redox mediators between an immobilized enzyme molecule and the electrode surface. Proteins can be immobilized following several strategies like covalent binding, physical adsorption or encapsulation within inert matrices [8–10]. Among the available encapsulating agents, silica synthesized from sol-gel methodologies provides soft immobilization conditions and offers protection against some bulk solution components, thus reducing the risk of denaturation because of pH or ionic strength effects[11–15]. Following this approach, we have employed silica to immobilize the redox active protein cytochrome c (cyt c).

Cyt c is a water soluble hemoprotein, with an electron-transducing role in the biological respiratory chain, that has been used in several bioelectrochemical devices [16–18]. Paired with cytochrome oxidase it has been employed in biofuel cell cathodes [19,20] and, thanks to its direct activity as a peroxidase, also in biosensors [21–29]. Indeed, cyt c can be used in combination with other enzymes, such as the xanthine oxidase, to take advantage of its redox activity in the development of new biosensors [30–34].

Direct electrochemistry from cyt c to surface-modified metal electrodes or metal oxides electrodes has been also reported. The electron transfer is promoted by the attractive interaction of positively charged lysine moieties to surfaces [35]. Several studies on this topic were performed using transparent indium-doped tin oxide electrodes by Bowden and coworkers [36–39]. In early studies they pointed out

that the electron transfer rate to cyt c in solution depends on both electrode pretreatment and protein concentration. The magnitude of the heterogeneous rate constant was found to decrease as the cyt c concentration increased[38,39]. Cyt c can be adsorbed by these electrodes while retaining its native state and, therefore, its electroactivity[36,40–44].

In a previous contribution [45], we demonstrated that interactions between silica gel and encapsulated cyt c electrodes are relevant for an optimization of the electron-transfer to ITO electrodes. We found that methyl-modified silica lowers the affinity between negatively charged silica pores and protein molecules. The optimum organosilica film contains 20-30% methyl groups and promotes the detachment of the positively charged cyt c from the pores, thus positioning the redox center towards the electrode surface.

It is recognized that silica constitutes a suitable inert matrix for the encapsulation of several biomolecules[11,46–49]. However, this material presents a serious drawback from an electrochemical point of view, which is the lack of intrinsic electron conductivity. For that reason, the electrochemical response of cyt c encapsulated in silica is restricted to those protein molecules placed at pores nearby the electrode surface[45]. As a result, it is thought that the thicker the silica layer, the higher the amount of isolated cyt c showing no redox activity.

We faced the problem of using electrically insulating silica matrices in previous works[50–52]. There, we performed the encapsulation of highly electrocatalytic single-walled carbon nanotubes within silica (SWCNT@SiO_2). Such materials showed good electrochemical performance, which even improved the heterogeneous rate transfer for several redox probes. However, this was followed by a minor increase in the true electroactive area because most SWCNTs remained isolated into the silica network and were not electrically connected with the supporting electrode [53]. A conducting polymer was then

inserted within the silica pores to wire the electrode surface to the isolated nanotubes[50,51] and the result was a hybrid silica material with improved electrocatalytic performance[52].

Several strategies can be followed to improve the electrical connection between encapsulated proteins and substrate electrodes through different nanostructured materials, including metal nanoparticles, carbon nanotubes, metallic or molecular nanowires [54–57]. In the present work we propose a different method for the electrical activation of the encapsulated protein, which involves the insertion of conducting polymer wires through the pores of silica. The goal is to improve the electron transfer between electrode surface and cyt c encapsulated within a methyl-modified silica matrix. Since part of the protein molecules remain in isolated locations of the silica layer after encapsulation, we will wire them to the electrode surface by means of the electrochemical insertion of a conducting polymer (PEDOT/PSS).

2. Experimental section

Cytochrome c (Cyt c) from horse heart (98%), 3,4-ethylendioxythiophene (EDOT) (97%), poly(sodium 4-styrenesulfonate) (PSS) (p.a.), tetraethyl orthosilicate (TEOS) and triethoxy(methyl)silane (MTES) were purchased from Sigma-Aldrich. Hydrochloric acid (p.a.) was purchased from VWR-Chemicals. Potassium dihydrogen phosphate (p.a.) and dipotassium hydrogen phosphate (p.a.) were from Merck. All the aqueous solutions were prepared using ultrapure water from an Elga Labwater Purelab system (18.2 MΩ cm).

Cyclic voltammetry was performed with a potentiostat (Elektronik Potentiostat Wenking ST 72, Bank Elektronik Germany), a wave programmer (EG&G PARC) and a digital recorder (eDAQ - 410), with eDAQ EChart data acquisition software. The electrochemical cell was purged by bubbling a N_2 flow

for 20 min in the solution, and the N_2 atmosphere was maintained during the whole experiment. A platinum wire has been used as a counter electrode and indium-tin oxide glass substrate (ITO Delta, CG-60IN, 60 S cm^{-1}) were used as working electrodes. Before using it, the ITO glass was degreased by sonication in an acetone bath and rinsed with an excess of deionized water. A working electrode with a geometric area of 1 cm^2 was immersed in the solution for each electrochemical characterization. The electroactive area of ITO modified electrodes was determined from the measurement of the double layer charge. A reversible hydrogen electrode (RHE) immersed in the same electrolyte solution within a Luggin capillary was used as the reference electrode.

UV-Visible spectra were acquired with a JASCO V-670 spectrophotometer. UV-vis spectroelectrochemical experiments were performed with a bipotentiostat/galvanostat (*μStat 400 DropSens*) with *DropView* data acquisition software. The spectroelectrochemical cell was a conventional quartz cell (1 cm optical path) with a Teflon cap to fit an ITO/glass working electrode, a silver wire pseudoreference electrode and a platinum wire as a counter electrode. The spectroelectrochemical cell was purged by bubbling an Ar flow for 10 min through the solution and Ar atmosphere was maintained during all the experiments.

For the synthesis of the silica-modified electrodes containing cyt c, two stock solutions were prepared as follows:

Solution 1, Methyl-modified silica precursor solution was prepared by mixing 1.48 mL TEOS (6.63 mmol) and 0.464 mL MTES (2.33 mmol) with 2.983 mL HCl (0.01 M) under magnetic stirring conditions at room temperature during two hours in a closed vial. Then the resulting solution was

rota-evaporated until the complete removal of the stoichiometric amount of ethanol released from the hydrolysis reaction.

Solution 2, cytochrome c solutions with concentration ranging between 10-100 mg mL^{-1} were prepared by dissolving the protein in a phosphate buffer solution (PBS, pH 7) made of K_2HPO_4 0.15M + KH_2PO_4 0.1M.

For the encapsulation and immobilization of cytochrome c on the electrode 20 μL of *solution 1* plus 20 μL of *solution 2* were placed in an Eppendorf vial. The concentration of cytochrome c in this silica solution ranged from 5 to 50 mg mL^{-1}. 20 μL of this mixture was dispensed over a clean ITO electrode. After a time period of 20-40 s a homogeneous silica gel containing cyt c is formed over the ITO surface.

For simplicity, the mass of cyt c loaded in the silica gel has been used to label each material. For example, the electrode prepared from a precursor solution containing 10 mg mL^{-1} of protein is labelled as cyt c(0.2 mg)@$SiO_{1.87}Me_{0.26}$.

The electropolymerization of PEDOT-PSS was performed by the potentiodynamic method in an aqueous solution containing 0.15% PSS + 45 mM EDOT monomer. The mixture was sonicated for 10 min to dissolve the monomer.

3. Results and discussion

The hydrophobic, partially methylated silica matrix has been evaluated as an electron-transfer immobilization host for cyt c. Fig. 1.a shows cyclic voltammograms recorded in a pH 7 phosphate

buffer solution at several hemoprotein loadings. Solid line in Fig. 1.a shows the electrochemical response of the cyt c(0.2 mg)@$SiO_{1.87}Me_{0.26}$ electrode.

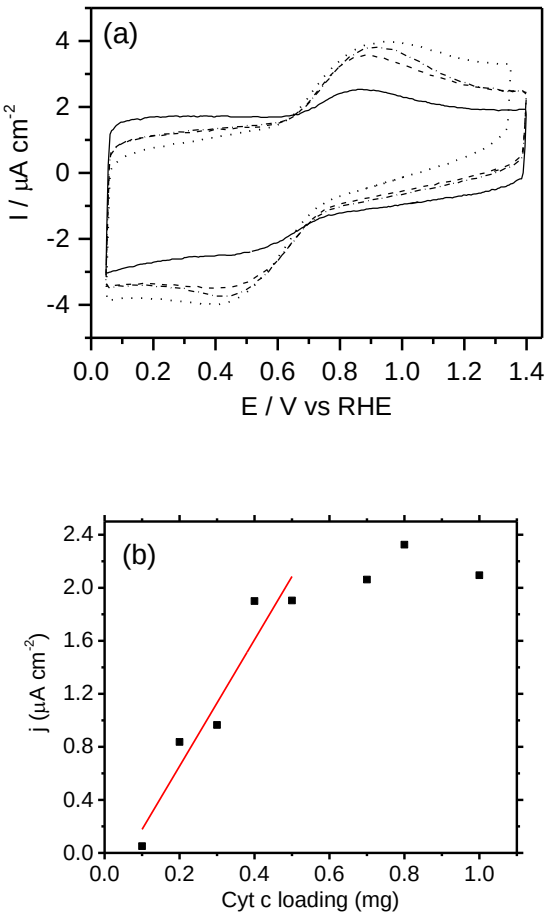

Figure 1. (a) Cyclic voltammograms for cyt c encapsulated in a silica matrix, cyt c(x mg) @$SiO_{1.87}Me_{0.26}$, and recorded for different protein loadings in the gel (—) x= 0.2; (– – –) x= 0.4; (– · –) x= 0.7; (·····) x= 1.0 mg. Electrolytic medium: pH 7 PBS. Scan rate 100 mV s^{-1}. **(b)** Peak current density versus concentration of cyt c in the precursor solution. Obtained from a CV set as in (a).

The anodic peak centered at 0.86 V during the forward potential scan is related to the oxidation of ferrocytochrome c to ferricytochrome c. The reverse scan shows the reduction counter process, which appears as a cathodic feature peaking at around 0.47 V.

Fig. 1.a also shows the stabilized voltammograms recorded at increasing loadings of cyt c. As expected, oxidation-reduction peak currents rise at increasing amounts of encapsulated cyt c and, simultaneously, the associated voltammetric waves become more defined.

The current intensity of the encapsulated cyt c peaks were analysed for a cyt c@$SiO_{1.87}Me_{0.26}$ electrodes by plotting the logarithm of the current intensity versus the logarithm of the sweep rate in a PBS solution (see Fig. S1 in the Supporting Information). The slope of the linear fit is close to 0.5, which means a peak current nearly proportional to square root of the scan rate. Similar results were obtained for different protein loadings. In this way, despite that cyt c is encapsulated, its electrochemical behaviour resembles that of a free species in solution. It can be then inferred that the silica host allows a certain mobility of proteins within its pores.

The evolution of anodic peak currents was plotted against the amount of cyt c incorporated in silica in Fig. 1.b for a number of samples. There, it can be observed that peak currents are proportional to the amount of cyt c up to a value of 0.5 mg within the gel. Higher protein loadings seem not to affect significantly the recorded current, which reaches a constant value.

In order to compare the amount of electroactive protein with the total protein encapsulated within the silica matrix, we performed a deeper analysis of voltammetric results. The evolution of the redox current intensity as a function of the scan rate were examined. To estimate the apparent concentration of encapsulated protein we can make use of the Randles-Sevcik equation

$$I_p = 2.687x10^5 ACn^{3/2}(Dv)^{1/2}$$

being C the concentration of protein (mol cm^{-3}), A the electroactive area of the electrode (cm^2), D the diffusion coefficient of encapsulated protein (4.7×10^{-7} cm^2 s^{-1} within the silica gel [45]) and ν the scan rate (V s^{-1}).

From this equation, the apparent concentration of electroactive cyt c is in the order of 10^{-5} M for all the electrodes tested (the values of electroactive cyt c relative to the total amount of encapsulated protein are presented in Fig. S2 of the Supporting Information).

It can be observed that the amount of electroactive protein is much smaller than the encapsulated one (indeed, only of the 2% protein shows electroactivity). This suggests that most cyt c molecules are located within isolated pores or, alternatively, they underwent some kind of modification (oligomerization, aggregation, etc.)[58,59] making them inactive.

The voltammetric peak-to-peak separation was also studied by the Nicholson method in order to obtain heterogeneous transfer rate constants (k^o) [60] for the different electrodes containing cyt c. Fig. 2 shows k^o values for different amounts of encapsulated protein.

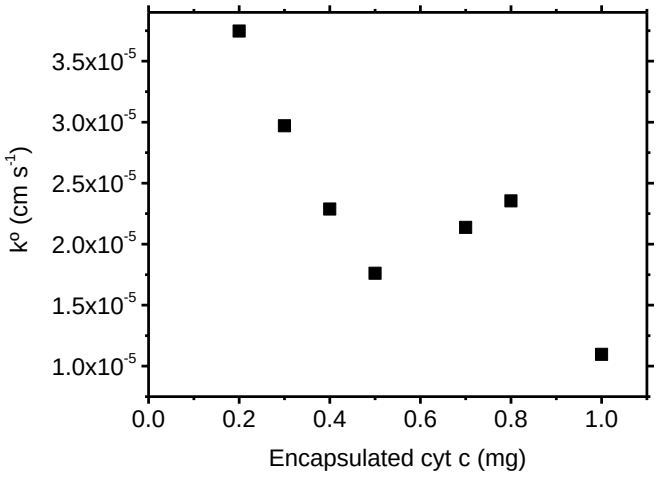

Figure 2: Heterogeneous rate constant calculated from voltammetric data for the redox reaction of cyt c encapsulated in silica.

Low k^o values were obtained (in the order of 10^{-5} cm s^{-1}) that may reveal high affinity of silica pores to cyt c for the heme group that may hinder the transfer to the ITO surface. In a previous work [45] we detected that the presence of OH-terminated silica pores results in a lack of redox response from encapsulated protein. However, the insertion of methyl functionalities in the silica structure reduced the pore-cyt c interaction and allowed the observation of the electrochemical response of encapsulated cyt c.

On the other hand, as shown by Runge et al. [42] , the presence of silica can disturb the orientation of cyt c with respect to the electrode surface, thus decreasing the efficiency of the electron transfer.

It is also worth mentioning that increasing amounts of encapsulated cyt c lead to a decrease in the value of the transfer constant. This effect of cyt c concentration on k^o was already observed for several

electrodes [38,61]. k^o decrease almost one order of magnitude at bare ITO after changing cyt c concentration from 38 to 300 µM [38]. These values are well below the concentration range employed in the present work (400 µM to 4 mM), so we expect lower k^o figures (in the order of 10^{-5} cm s^{-1}), which are compatible with the work by Marten and McKenzie [59]. For cyt c concentrations up to 53 mM at titania membranes deposited on ITO, k^o values were in the order of 10^{-6} cm s^{-1}. There, the formation of cyt c aggregates and the electron transfer through a "hopping" mechanism were at the origin of the low k^o values. Similar hopping mechanism was reported by Beissenhirtz et al. for cyt c multilayers assembled within a polyelectrolyte film [62].

In our case, the existence of a limiting load value of cyt c at around 0.5 mg strongly suggests that there is an increasing excess of electroactive molecules residing in non-accessible sites of the silica matrix. Then, a strategy to connect those electroactive yet isolated cyt c molecules to the electrode surface by means of a suitable conducting polymer will be developed.

It is known that conducting polymers can be inserted into the pores of host silica matrices by means of electrochemical methods. The usual technique involves either a potentiostatic or potentiodynamic polymerization of the selected monomer on a working electrode previously covered by the silica layer[50–52].

First, we will show the electrochemical response of a $SiO_{1.87}Me_{0.26}$ layer recorded in aqueous solution containing 45 mM EDOT monomer and 0.15% PSS (Fig. 3)

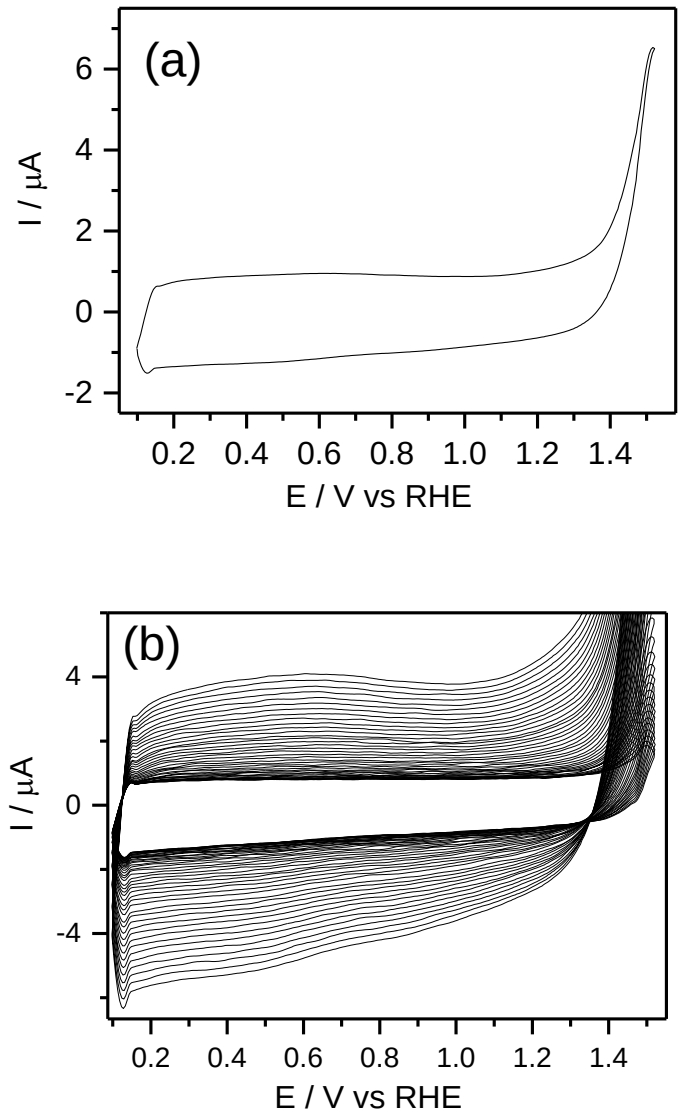

B

Figure 3: Cyclic voltammograms recorded for a $SiO_{1.87}Me_{0.26}$ layer deposited on ITO in 45 mM EDOT + 0.15% PSS aqueous solution. a) First potential cycle; b) 35 subsequent cycles. Scan rate 100 mV s^{-1}.

During the first forward scan (Fig. 3.a) an anodic current develops from 1.3 V corresponding to the oxidation of EDOT monomer. As a result of the electrochemical reaction, a current plateau grows continuously within the 0.1 - 1.1V potential region during successive potential scans, as observed in

Fig 3.b. This featureless current extending up to 1.1 V is characteristic of a pseudocapacitative process occurring at the deposited polymer in its conducting state. The current intensity can be used to estimate the amount of polymer inserted within the silica layer, assuming a mass capacitance of 67.7 F g^{-1}, as determined by Bobacka *et al.*[63]. The double layer capacitance was determined from voltammetric measurements of currents at potentials between 0.2-0.5V.

The electropolymerization of PEDOT across a silica material previously loaded with protein, cyt c(0.5 mg)@$SiO_{1.87}Me_{0.26}$, shows marked differences against the cyclic voltammograms in Fig 3. The Electropolymerization of PEDOT across this electrode cyt c is shown in Fig. 4.

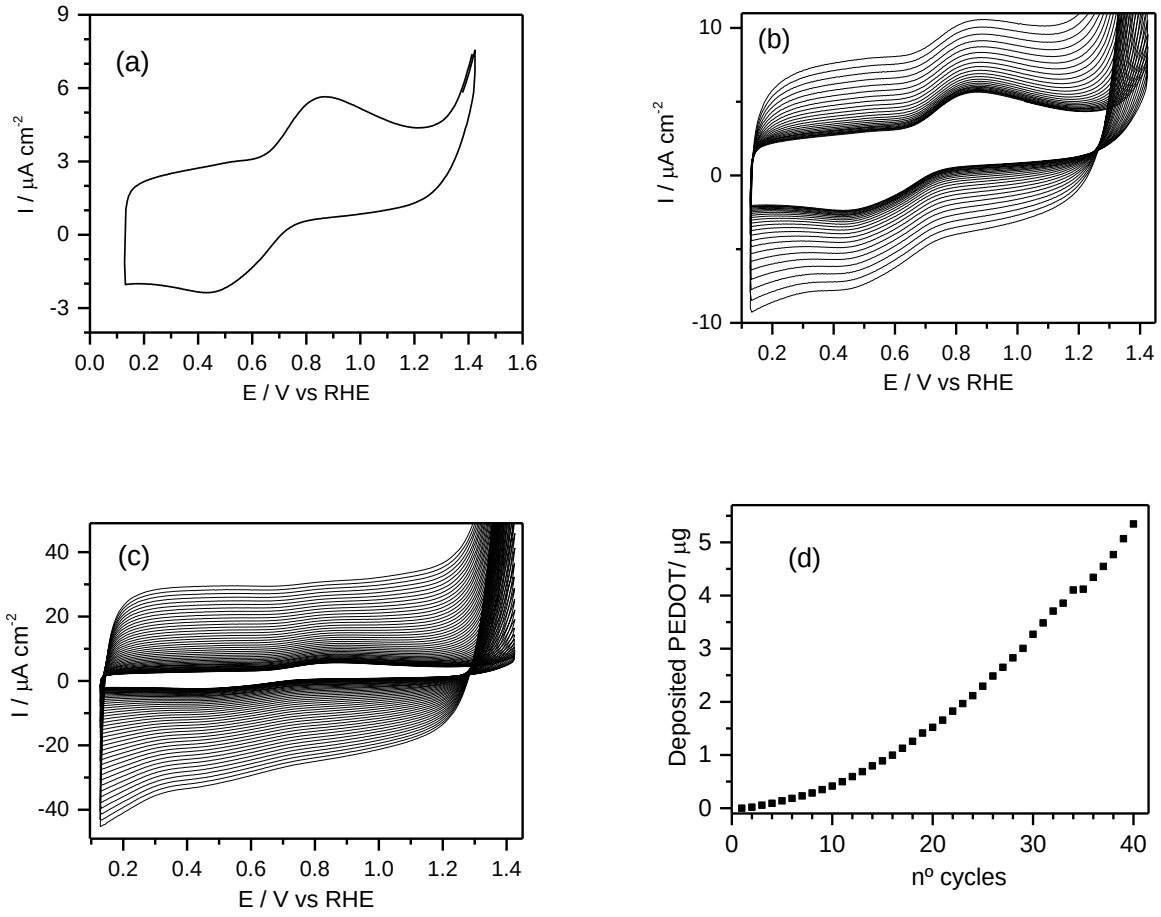

Figure 4. (a) First voltammetric cycle showing the potentiodynamic growth of a PEDOT film over a cyt c (0.5 mg)@$SiO_{1.87}Me_{0.26}$ material. **(b)** 2^{nd} -24^{th} cycle and **(c)** 25^{th}-40^{th} cycle. Polymerization conditions: [EDOT] = 45 mM; [PSS]= 0.15% (w/w). Background electrolyte: pH 7 phosphate buffer. Scan rate 100 mV s^{-1}. **(d)** Plot showing the mass of PEDOT deposited into the cyt c(0.5 mg)@$SiO_{1.87}Me_{0.26}$ material at increasing number of potential cycles up to 1.4 V.

The first voltammetric scan (Fig. 4.a) shows two separate electrochemical processes. The first one is a pair of redox peaks (0.87 V/ 0.43 V) that can be clearly ascribed to the reversible oxidation of iron centers at cyt c molecules. The second one corresponds to EDOT monomer oxidation, which occurs at potentials above 1.3 V. After several potential cycles in the 0.1-1.4 V potential range (shown in Figs. 4b and 4c) the monomer oxidation process gives rise to the insertion of the corresponding electroactive polymer (PEDOT) within the silica matrix pores.

The pair of peaks associated with the redox process of cyt c is discernible during, roughly, the 25 first scans. From that point, the overlapping of PEDOT redox currents makes it difficult to recognize the cyt c voltammetric features (see Fig. 4c). The mass of inserted polymer was estimated from the pseudocapacitative current in the 0.2-0.5V potential range and it has been depicted against the number of polymerization cycles in Fig. 4d. The shape of this plot suggests an autocatalytic growth of the polymer inside the silica matrix, as it has been already reported [64,65].

UV-vis spectroscopy has been widely employed in the literature to characterize the oxidation state of cyt c[66,67] and we have performed electrochemical *in situ* experiments of cyt c(0.5 mg)@$SiO_{1.87}Me_{0.26}$ with the same purpose. The characteristic spectra of cyt c does not undergo substantial modifications after the encapsulation within the gel (see fig. S3 in the Supporting information). Particularly, it is observed that the Soret band does not shift, revealing that the protein remains native when encapsulated [45]. Fig. 5 shows two UV-Vis spectra corresponding to electrochemical oxidized and reduced cyt c encapsulated in silica and immersed in PBS medium.

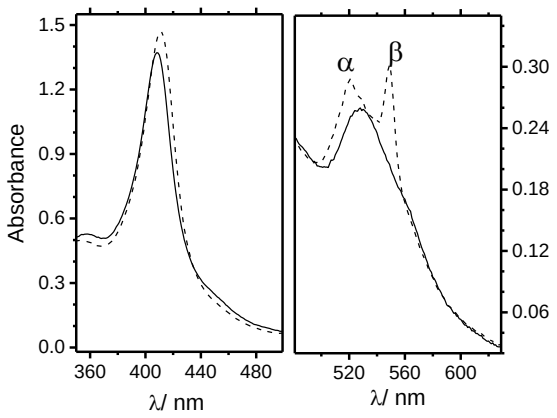

Figure 5. (a) *In situ* UV-Vis spectra collected for a cyt c(0.5 mg)@$SiO_{1.87}Me_{0.26}$ in PBS. Static spectra acquired at 1.1V (solid line) and 0.3 V (dashed line)

The spectrum of oxidized ferricytochrome c was acquired at 1.1 V, where the protein is in its native form. It is characterized by the ππ* electronic transitions of the porphyrin group with an intense Soret band in the region between 380 and 460 nm and poorly defined lower energy Q-bands at around 500-570 nm. On the other hand, the spectrum of reduced ferrocytochrome c was collected at 0.3 V. There, the Soret band shifts to red and intensifies slightly, while the Q band splits into two well-defined features, the so-called α and β bands, peaking at 520 and 549 nm, respectively.

The conventional absorption spectra presented in Fig. 5 cannot be used to gain accurate time-resolved information from the investigated system because the absolute intensity change is too low. Therefore, to make clear the effect of time on the electrochemical reduction treatment, we have presented in Fig. 6 normalized differential UV-Vis spectra, $\Delta A/A_0$.

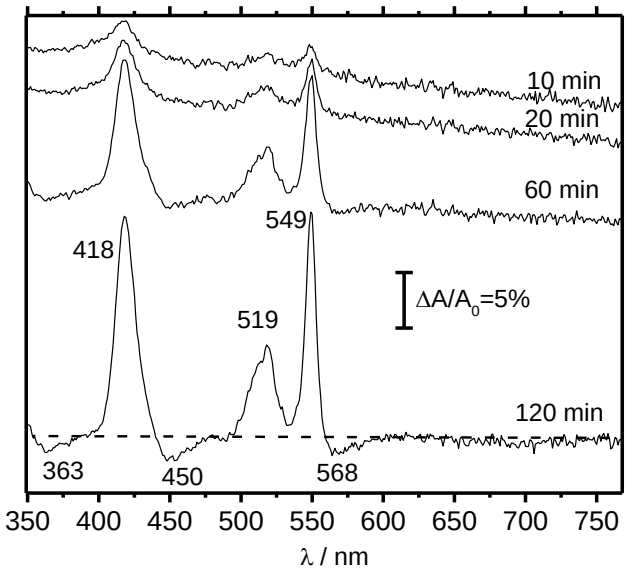

Figure 6. *In situ* UV-Vis differential absorption spectra collected for a cyt c (0.5 mg)@$SiO_{1.87}Me_{0.26}$ electrode in PBS medium at different times after the application of a 0.3 V pulse (Sample potential). Reference potential 1.1V

To achieve this, each absolute spectrum collected at the sample reduction potential (0.3 V) was referred to the initial spectrum obtained at the reference potential (1.1 V) and then normalized with the reference signal. Working in this way, upward (positive) bands in the computed spectrum reveal the promotion of new electronic transitions at the sample potential (0.3 V) that were absent at the reference potential and, besides, the evolution of spectra with time is clarified. As observed in Fig. 6, three positive absorption features develop at 418, 519 and 549 nm while negative bands appear clearly

at 363, 450 and 568 nm after 120 min reduction treatment. It is worth noting that the bipolar character observed for the electronic transitions in the spectral region of the Soret band is an artifact that comes from the potential-induced red shift of this band in the original absolute spectra.

Thanks to the differential spectra, we are now in position to assess the ability of PEDOT/PSS to transfer charge to cyt c molecules at non-accessible sites of the methylated silica matrix. In this way, an experiment parallel to that shown in Fig. 6 was performed for an electrode containing 6.45 μg of PEDOT, cyt c (0.5 mg)-PEDOT@$SiO_{1.87}Me_{0.26}$.

Fig. 7 shows the differential UV-Vis absorption bands acquired during the electrochemical reduction of cyt c at 0.3 V, where sample spectra are referred to the initial spectrum collected at 1.1 V. As in the previous experiment, the obtained bands are related with the effective reduction of the iron group. It can be observed a faster growth of these bands for the electrode containing PEDOT (note the different scale of the value axis in Fig. 6). Apart from this observation, there is another outstanding difference between both figures, which is the baseline distortion at wavelengths above 600 nm in Fig. 7. This element reveals the existence of polaron electronic transitions in the conducting polymer component at the reference potential that are absent in the cyt c@$SiO_{1.87}Me_{0.26}$ system. The absolute spectra of reduced and oxidized PEDOT are shown in the Supporting Information (Fig. S4).

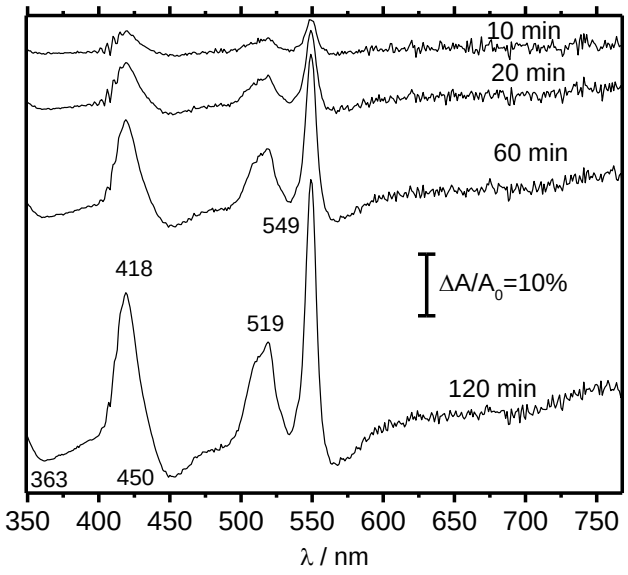

Figure 7. *In situ* UV-Vis differential absorption spectra collected in PBS medium at increasing times for a cyt c-PEDOT@$SiO_{1.87}Me_{0.26}$ (6.45 µg polymer inserted) after the application of a sample reduction potential of 0.3 V. Reference potential 1.1V

To disclose the effect of PEDOT on the rate of protein reduction it is required to monitor absorption intensity changes in the absence and in the presence of this conducting polymer. As observed in Fig. 7, the intensity of the β peak at 549 nm is particularly sensitive to the redox state of the iron center and such feature makes this band very useful for our purpose.

The band intensity recorded for the peak at 549 nm has been plotted in Fig. 8.a against the reaction time at 0.3 V. For comparison, this figure shows also the behavior of the *β* band in a parallel experiment performed with a cyt c@$SiO_{1.87}Me_{0.26}$ electrode with no PEDOT inserted.

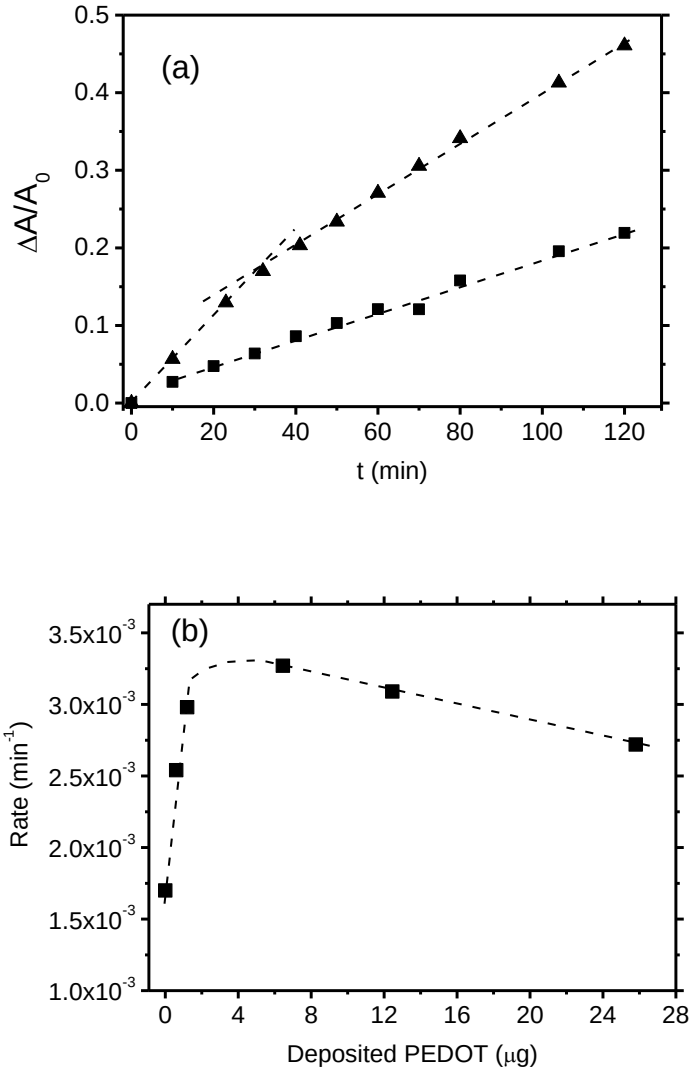

Figure 8. (a) Time dependence of the differential absorption band (sample potential 0.3V, reference potential 1.1V) at 549 nm for a cyt c(0.5 mg) @$SiO_{1.87}Me_{0.26}$ electrode. Square symbols correspond to an electrode without PEDOT, triangles correspond to an electrode containing 6.45 μg PEDOT inserted. **(b)** Shift rate of the 549 nm electronic absorption against the amount of PEDOT inserted.

The band intensity rises linearly at increasing times and shows a shift rate close to 1.7×10^{-3} min^{-1} in the absence of PEDOT. However, for the electrode containing PEDOT, two well-defined trends are observed. At short times, the shift rate is about to 5×10^{-2} min^{-1} but, after a transient period of 30 minutes, data can be fitted with a linear trend showing lower slope. The same behavior is observed for other samples containing different amounts of PEDOT in the range 0.6-25.8 μg. Interestingly, during the initial stages of electrochemical reduction (up to 30 min) it was found that shift rates are almost independent of the amount of PEDOT loaded. On the contrary, after this transient period, different linear trends with slopes strongly dependent on the PEDOT loading are observed. These slopes are plotted against the amount of PEDOT in Fig. 8.b. There, it is observed that the shift rate increases sharply at low polymer loadings, then it passes through a maximum value of 3.3×10^{-3} min^{-1} for a moderate 6.5 μg PEDOT loading and, finally, declines slightly for higher weights of inserted polymer.

Owing to the high complexity of the studied system, which involves species such as cyt c, PEDOT, PSS and the silica layer, the analysis of the observed drop occurring, roughly, above 8 μg PEDOT is not straightforward. Despite this, two are the most reasonable hypothesis that could explain this behavior. On the one hand, the high amount of PEDOT-PSS filling the silica pores may restrict the free movement of cyt c, causing a growing number of these molecules not to settle adequately for the charge transfer[68]. On the other hand, the existence of a vertical conductivity gradient at inserted PEDOT masking the results should not be ruled out. Those silica pores away from the ITO substrate (i.e. closer to the electrolyte solution) are richer in counteranions than inner pores. Since the electrochemical reduction at 0.3 V promotes the cutback of positively charges along the polymer

chain, the different amount of available negative charge could promote a conductivity alteration perpendicular to the electrode substrate. It is not easy to discern between these two possibilities but, undoubtedly, the shift rate in Fig. 8.b is related with the effective population of cyt c transferring charge to the electrode. Therefore, it is derived that a moderate amount of inserted PEDOT is suitable to reach most of those formerly inactive (isolated) protein molecules showing no other detrimental effects.

4. Conclusions

We have studied the direct electron transfer between ITO electrodes and cytochrome c molecules encapsulated within partially methylated silica matrices ($SiO_{1.87}Me_{0.26}$). As expected, it was found that increasing the amount of cyt c results in higher peak currents related with the redox transformation of the protein iron center. However, the proportionality between immobilized cyt c amount and recorded redox current breaks at high cyt c loadings. This observation strongly suggests that a portion of the encapsulated electroactive protein actually exists in non-accessible sites of the dielectric silica matrix. The electrochemical insertion of a conducting polymer (PEDOT) through the silica matrix proved a successful strategy to connect the electrode surface with those formerly isolated protein molecules.

The kinetics of the electron transfer between protein and ITO electrode was followed by *in situ* UV-vis spectroelectrochemical experiments. The presence of PEDOT inside the silica produced up to a 3-fold enhancement in the protein reduction rate. However, it was demonstrated that the amount of inserted polymer plays a significant role on the electrochemical reduction rate. Small and moderate

loadings resulted in better performance than higher PEDOT loadings, probably due to the restriction imposed by the conducting polymer to the free movement of cyt c, since a suitable orientation of the iron redox center is required for the charge transfer. The presence of low conductivity domains in the PEDOT material could be also at the origin of the observed effect and this possibility should not be ruled out. For a film containing 0.5 mg protein, the best electrochemical reduction rate was obtained after the insertion of 6.45 μg PEDOT, a value that corresponds to 1.1 units of EDOT monomer per cyt c molecule.

5. Acknowledgment

Financial support from the Spanish Ministerio de Economía y Competitividad and FEDER funds (MAT2013-42007-P) and from the Generalitat Valenciana (PROMETEO2013/038) is gratefully acknowledged.

6. References

(1) Kim, J.; Jia, H.; Wang, P. *Biotechnol. Adv.* **2006**, *24* (3), 296–308.

(2) Cooney, M. J.; Svoboda, V.; Lau, C.; Martin, G.; Minteer, S. D. *Energy Environ. Sci.* **2008**, *1* (3), 320.

(3) Ivnitski, D.; Branch, B.; Atanassov, P.; Apblett, C. *Glucose oxidase anode for biofuel cell based on direct electron transfer*; 2006; Vol. 8.

(4) Leech, D.; Kavanagh, P.; Schuhmann, W. *Electrochim. Acta* **2012**, *84*, 223–234.

(5) Walcarius, A.; Minteer, S. D.; Wang, J.; Lin, Y.; Merkoçi, A. *J. Mater. Chem. B* **2013**, *1* (38), 4878.

(6) Villalonga, R.; Díez, P.; Yáñez-Sedeño, P.; Pingarrón, J. M. *Electrochim. Acta* **2011**, *56* (12),

4672–4677.

(7) Pita, M.; Gutierrez-Sanchez, C.; Toscano, M. D.; Shleev, S.; De Lacey, A. L. *Bioelectrochemistry* **2013**, *94*, 69–74.

(8) Poulos, N. G.; Hall, J. R.; Leopold, M. C. *Langmuir* **2015**, *31* (4), 1547–1555.

(9) Sassolas, A.; Blum, L. J.; Leca-Bouvier, B. D. *Biotechnol. Adv.* **2012**, *30* (3), 489–511.

(10) Sheldon, R. A.; van Pelt, S. *Chem. Soc. Rev.* **2013**, *42* (15), 6223–6235.

(11) Esquembre, R.; Poveda, J. A.; Mateo, C. R. *J. Phys. Chem. B* **2009**, *113* (21), 7534–7540.

(12) Nadzhafova, O.; Etienne, M.; Walcarius, A. *Electrochem. commun.* **2007**, *9* (5), 1189–1195.

(13) Wang, Z. J.; Etienne, M.; Quiles, F.; Kohring, G. W.; Walcarius, A. *Biosens. Bioelectron.* **2012**, *32* (1), 111–117.

(14) Walcarius, A. *Anal. Bioanal. Chem.* **2010**, *396* (1), 261–272.

(15) Sassolas, A.; Blum, L. J.; Leca-Bouvier, B. D. *Sensors and Actuators B-Chemical* **2009**, *139* (1), 214–221.

(16) Lisdat, F.; Dronov, R.; Möhwald, H.; Scheller, F. W.; Kurth, D. G. *Chem. Commun.* **2009**, *552* (3), 274–283.

(17) Jin, W.; Brennan, J. D. *Anal. Chim. Acta* **2002**, *461* (1), 1–36.

(18) Tang, Y.; Dave, B. C. *Adv. Mater.* **1998**, *10* (18), 1536–1540.

(19) Katz, E.; Willner, I. *J. Am. Chem. Soc.* **2003**, *125* (22), 6803–6813.

(20) Haas, A. S.; Pilloud, D. L.; Reddy, K. S.; Babcock, G. T.; Moser, C. C.; Blasie, J. K.; Dutton, P. L. *J. Phys. Chem. B* **2001**, *105* (45), 11351–11362.

(21) Wang, G.-X.; Qian, Y.; Cao, X.-X.; Xia, X.-H. *Electrochem. commun.* **2012**, *20*, 1–3.

(22) Gómez-Mingot, M.; Iniesta, J.; Montiel, V.; Kadara, R. O.; Banks, C. E. *Analyst* **2011**, *136* (10), 2146.

(23) Ge, B.; Lisdat, F. *Anal. Chim. Acta* **2002**, *454* (1), 53–64.

(24) Lvovich, V.; Scheeline, A. *Anal. Chem.* **1997**, *69* (3), 454–462.

(25) Cortina-Puig, M.; Muñoz-Berbel, X.; Calas-Blanchard, C.; Marty, J.-L. *Talanta* **2009**, *79* (2), 289–294.

(26) Beissenhirtz, M. K.; Scheller, F. W.; Lisdat, F. *Anal. Chem.* **2004**, *76* (16), 4665–4671.

(27) Lisdat, F.; Ge, B.; Ehrentreich-Förster, E.; Reszka, R.; Scheller, F. W. *Anal. Chem.* **1999**, *71* (7), 1359–1365.

(28) Scheller, W.; Jin, W.; Ehrentreich-Förster, E.; Ge, B.; Lisdat, F.; Büttemeier, R.; Wollenberger, U.; Scheller, F. W. *Electroanalysis* **1999**, *11* (10-11), 703–706.

(29) Eguílaz, M.; Agüí, L.; Yáñez-Sedeño, P.; Pingarrón, J. M. *J. Electroanal. Chem.* **2010**, *644* (1), 30–35.

(30) Kakehi, N.; Yamazaki, T.; Tsugawa, W.; Sode, K. *Biosens. Bioelectron.* **2007**, *22* (9), 2250–2255.

(31) Pastor, I.; Esquembre, R.; Micol, V.; Mallavia, R.; Mateo, C. R. *Anal. Biochem.* **2004**, *334* (2), 335–343.

(32) Dronov, R.; Kurth, D. G.; Möhwald, H.; Scheller, F. W.; Lisdat, F. *Electrochim. Acta* **2007**, *53* (3), 1107–1113.

(33) Cortina-Puig, M.; Scangas, A. C. H.; Marchese, Z. S.; Andreescu, S.; Marty, J.-L.; Calas-Blanchard, C. *Electroanalysis* **2010**, *22* (20), 2429–2433.

(34) Gill, I.; Ballesteros, A. *Trends Biotechnol* **2000**, *18* (7), 282–296.

(35) Daido, T.; Akaike, T. *J. Electroanal. Chem.* **1993**, *344* (1-2), 91–106.

(36) El Kasmi, A.; Leopold, M. C.; Galligan, R.; Robertson, R. T.; Saavedra, S. S.; El Kacemi, K.; Bowden, E. F. *Electrochem. commun.* **2002**, *4* (2), 177–181.

(37) Nakano, K.; Yoshitake, T.; Yamashita, Y.; Bowden, E. F. *Langmuir* **2007**, *23* (11), 6270–6275.

(38) Bowden, E. F.; Hawkridge, F. M.; Chlebowski, J. F.; Bancroft, E. E.; Thorpe, C.; Blount, H. N. *J. Am. Chem. Soc.* **1982**, *104* (26), 7641–7644.

(39) Bowden, E. F.; Hawkridge, F. M.; Blount, H. N. *J. Electroanal. Chem. Interfacial Electrochem.* **1984**, *161* (2), 355–376.

(40) Willit, J. L.; Bowden, E. F. *J. Electroanal. Chem. Interfacial Electrochem.* **1987**, *221* (1-2), 265–274.

(41) Runge, A. F.; Saavedra, S. S. *Langmuir* **2003**, *19* (22), 9418–9424.

(42) Runge, A. F.; Mendes, S. B.; Saavedra, S. S. *J. Phys. Chem. B* **2006**, *110* (13), 6732–6739.

(43) Renault, C.; Andrieux, C. P.; Tucker, R. T.; Brett, M. J.; Balland, V.; Limoges, B. *J. Am. Chem. Soc.* **2012**, *134* (15), 6834–6845.

(44) Schaming, D.; Renault, C.; Tucker, R. T.; Lau-Truong, S.; Aubard, J.; Brett, M. J.; Balland, V.; Limoges, B. *Langmuir* **2012**, *28* (39), 14065–14072.

(45) Gamero-Quijano, A.; Huerta, F.; Morallon, E.; Montilla, F. *Langmuir* **2014**, *30* (34), 10531–10538.

(46) Frenkel-Mullerad, H.; Avnir, D. *J. Am. Chem. Soc.* **2005**, *127* (22), 8077–8081.

(47) Wang, Z. J.; Etienne, M.; Kohring, G. W.; Walcarius, A. *Electroanalysis* **2010**, *22* (17-18), 2092–2100.

(48) Doherty, W. J.; Armstrong, N. R.; Saavedra, S. S. *Chem. Mater.* **2005**, *17* (14), 3652–3660.

(49) Ellerby, L. M.; Nishida, C. R.; Nishida, F.; Yamanaka, S. a; Dunn, B.; Valentine, J. S.; Zink, J. I. *Science (80-.).* **1992**, *255* (5048), 1113–1115.

(50) Montilla, F.; Cotarelo, M. A.; Morallón, E. *J. Mater. Chem.* **2009**, *19* (2), 305.

(51) Salinas-Torres, D.; Montilla, F.; Huerta, F.; Morallón, E. *Electrochim. Acta* **2011**, *56* (10),

3620–3625.

(52) Gamero-Quijano, A.; Huerta, F.; Salinas-Torres, D.; Morallon, E.; Montilla, F. *Electrochim. Acta* **2014**, *135*, 114–120.

(53) Gamero-Quijano, A.; Huerta, F.; Salinas-Torres, D.; Morallón, E.; Montilla, F. *Electrocatalysis* **2013**, *4* (4), 259–266.

(54) Willner, B.; Katz, E.; Willner, I. *Curr. Opin. Biotechnol.* **2006**, *17* (6), 589–596.

(55) Gooding, J. J.; Wibowo, R.; Liu, †; Yang, W.; Losic, D.; Orbons, S.; Mearns, F. J.; Shapter, J. G.; Hibbert, D. B. *J. Am. Chem. Soc.* **2003**, *125* (30), 9006–9007.

(56) Xu, J.; Shang, F.; Luong, J. H. T.; Razeeb, K. M.; Glennon, J. D. *Biosens. Bioelectron.* **2010**, *25* (6), 1313–1318.

(57) Jiménez, J.; Sheparovych, R.; Pita, M.; Narvaez García, A.; Dominguez, E.; Minko, S.; Katz, E. *J. Phys. Chem. C* **2008**, *112* (19), 7337–7344.

(58) Parui, P. P.; Deshpande, M. S.; Nagao, S.; Kamikubo, H.; Komori, H.; Higuchi, Y.; Kataoka, M.; Hirota, S. *Biochemistry* **2013**, *52* (48), 8732–8744.

(59) McKenzie, K. J.; Marken, F. *Langmuir* **2003**, *19* (10), 4327–4331.

(60) Gamero-Quijano, A.; Huerta, F.; Salinas-Torres, D.; Morallón, E.; Montilla, F. *Electrocatalysis* **2014**, 33–41.

(61) Reed, D. E.; Hawkridge, F. M. *Anal. Chem.* **1987**, *59* (19), 2334–2339.

(62) Beissenhirtz, M. K.; Scheller, F. W.; Stöcklein, W. F. M.; Kurth, D. G.; Möhwald, H.; Lisdat, F. *Angew. Chemie - Int. Ed.* **2004**, *43* (33), 4357–4360.

(63) Bobacka, J.; Lewenstam, A.; Ivaska, A. *J. Electroanal. Chem.* **2000**, *489* (1-2), 17–27.

(64) Prathish, K. P.; Carvalho, R. C.; Brett, C. M. A. *Electrochem. commun.* **2014**, *44*, 8–11.

(65) Nasybulin, E.; Wei, S.; Kymissis, I.; Levon, K. *Electrochim. Acta* **2012**, *78*, 638–643.

(66) Matsuda, N.; Santos, J. H.; Takatsu, A.; Kato, K. *Thin Solid Films* **2003**, *438-439* (03), 403–406.

(67) Dai, Y.; Zheng, Y.; Swain, G. M.; Proshlyakov, D. A. *Anal. Chem.* **2011**, *83* (2), 542–548.

(68) Wang, L.; Wang, E. *Electrochem. commun.* **2004**, *6* (1), 49–54.